

# Spin-wave nonreciprocity based on interband magnonic transitions

Kai Di<sup>1</sup>, Hock Siah Lim<sup>1</sup>, Vanessa Li Zhang<sup>1</sup>, Ser Choon Ng<sup>1</sup> & Meng Hau Kuok<sup>1</sup>

<sup>1</sup>Department of Physics, National University of Singapore, 2 Science Drive 3,  
Singapore 117542, Singapore.

## ABSTRACT

Nonreciprocal wave propagation is crucial to the stable operation of ultra-compact chips with low power consumption, and is the basis of unidirectional devices that are widely used in information technology and telecommunications. In the rapidly expanding fields of magnonics and magnon spintronics, spin waves, which are elementary excitations in ordered magnetic materials, act as information carriers. Numerous studies have been conducted on the manipulation and control of spin waves but, to our knowledge, none are devoted to their nonreciprocity at the nanoscale. Here, based on numerical simulations and a novel analytical coupled-mode theory of spin waves, we theoretically demonstrate linear nonreciprocal interband spin-wave mode transitions in a nanoscale waveguide, arising from time-reversal and space-inversion symmetry breaking by an applied magnetic field. Importantly, such spin-wave nonreciprocity could be realized at the nanoscale, thus facilitating magnonic nanodevice integration.

Keywords: spin-wave nonreciprocity, interband magnonic transition, coupled-mode theory of spin waves, signal isolation

Corresponding authors:

H.S.L. (Email: [phylimhs@nus.edu.sg](mailto:phylimhs@nus.edu.sg))

M.H.K. (Email: [phykmh@nus.edu.sg](mailto:phykmh@nus.edu.sg))

Besides being of scientific interest, the phenomenon of the nonreciprocal propagation of waves is of great technological importance. From the perspective of applications, nonreciprocity provides an extra degree of control in molding the flow of waves in fields ranging from mature microwave technology and laser optics to the rapidly growing areas of photonics[1-10], magnonics[11, 12] and phononics[13, 14]. Furthermore, it is crucial to the stabilization of integrated circuits and the suppression of undesirable crosstalk and interference arising from imperfection-induced scattering[4].

Nonreciprocal wave propagation generally entails the destruction of time-reversal symmetry. One common approach for realizing nonreciprocity is based on nonlinear effects and spatial asymmetry, but it is complicated and energy inefficient as it usually requires high wave intensities. Another approach utilizes certain materials which mediate coupling between waves propagating in them and an applied magnetic field (as in the Faraday effect), for which time-reversal symmetry is naturally broken by the field. However, this method suffers from the fact that generally the coupling is weak. In the past decade, many theoretical and experimental demonstrations have been carried out to achieve on-chip integration of wave nonreciprocity and isolation.

Spin waves are attracting growing research attention in the area of magnonics[15-24] of nanomagnets, due to attributes like their short wavelengths and highly tunable dynamic properties[17]. Because of their low energy dissipation, spin waves in magnetic insulators[16, 20-22] find applications in spintronics as an ideal spin current carrier. In these research fields, spin-wave nonreciprocity is important for various functionalities. For instance, Amiri *et al.*[11] studied the nonreciprocal dispersion and surface localization properties of spin waves in thin-film metallic ferromagnets, which could be employed in integrated microwave circuits. Sekiguchi *et al.*[12] reported the nonreciprocal emission of spin-wave packets in FeNi thin films which could be utilized to realize simple logic inputs of “1” and “0” in magnonic circuits. Very recently, An *et al.*[25] observed controllable unidirectional heat flow mediated by nonreciprocal spin waves, a phenomenon which could pave the way for heat technology based on spin currents. In all these cases, the magnetic excitations studied are the longer-wavelength magnetostatic surface waves rather than the nanoscale-wavelength exchange spin waves. Nonreciprocity of magnetostatic surface waves[26] originates from the lower symmetry at sample surfaces and dipole-dipole interactions rather than from the isotropic exchange interaction. However, in the sub-100nm range, spin waves are exchange-dominated and nonreciprocity arising from dipole-dipole interaction is less significant. Hence, nanoscale

miniaturization of magnonic devices necessitates the realization of the nonreciprocity of exchange-dominated spin waves.

However, to our knowledge, nonreciprocity of exchange-dominated spin waves has not been investigated. In this article, employing micromagnetic simulations and a newly-developed analytical coupled-mode theory of exchange spin waves, we demonstrate that nanoscale linear nonreciprocity of exchange-dominated spin waves[18] in a nanostripe waveguide can be achieved by the application of a time-reversal and space-inversion symmetry-breaking magnetic field. Spin waves propagating in the waveguide undergo interband transitions which are dependent on propagation direction, in analogy to nonreciprocal photonic transitions[3]. Such a nonreciprocity could lead to unidirectional magnonic devices, such as spin-wave isolators which serve as building blocks in integrated magnonics.

## Results

**Band structure and mode transition.** The spin-wave waveguide (Fig. 1a) considered here is an  $8\mu\text{m}$ -long  $\text{Ni}_{80}\text{Fe}_{20}$  (Permalloy) nanostripe of rectangular cross section, with a width  $w$  of 32 nm and a thickness of 4 nm. In equilibrium and in the absence of an external magnetic field, the stripe is assumed to be approximately uniformly magnetized along the  $x$ -axis. In this equilibrium magnetization, the waveguide exhibits reciprocity, as the reflection symmetry operation,  $x \rightarrow -x$ , leaves the waveguide and the equilibrium magnetization unchanged, while transforming the spin-wave wavevector from  $\mathbf{k}$  into  $-\mathbf{k}$ . Due to lateral confinement, the effective wavenumber of spin waves across the width is quantized[27], with their dynamic magnetizations having even- or odd-symmetry mode profiles across the width. Figure 1b shows the lowest and second lowest energy bands, with respective even and odd symmetry, of the spin-wave dispersion relations of the waveguide. For brevity, a spin-wave mode with angular frequency  $\omega_n$  and wavenumber  $k_n$  will be labeled  $[\omega_n, k_n]$ , where  $n = 1, 2$ .

It has been shown that in photonic structures, indirect photonic transitions[3, 9, 28], i.e., the simultaneous frequency and wavevector shifts of photons, can be induced by modulation of the dielectric constant of the structures, in analogy to indirect electronic transitions in solids. Similarly, indirect transitions between two spin-wave modes within the waveguide can be induced by a perturbation magnetic field  $h'$ , of frequency  $\Omega$  and wavevector  $Q$ , applied along the  $x$ -direction

$$h'(x, y, t) = h_0(y) \cos(Qx - \Omega t) \quad (1)$$

where the amplitude of the field is defined by  $\mu_0 h_0(y) = 0.05$  T for  $y < 0$ , and  $\mu_0 h_0(y) = 0$  T for  $y > 0$ ,  $\mu_0$  being the vacuum permeability (see Fig. 1a). Significant transition between two spin-wave modes will occur only if the phase-matching conditions, namely  $Q = k_2 - k_1$  and  $\Omega = \omega_2 - \omega_1$ , where 1 and 2 denote the respective initial and final modes, are approximately satisfied.

We have established that for only certain pairs of  $Q$  and  $\Omega$  values, will the phase-matching conditions be simultaneously satisfied for transitions between modes  $[\omega_1, k_1]$  and  $[\omega_2, k_2]$ , but not for those between mode  $[\omega_1, -k_1]$  and any other mode (see Fig. 1b). This means that mode transitions will occur only for one propagation direction, indicating that spin-wave propagation in the waveguide is nonreciprocal. Of note is that this nonreciprocity phenomenon is due to the breaking of time-reversal and spatial-inversion symmetry induced by the perturbation magnetic field.

**Coupled-mode model for exchange spin waves.** Here,  $\Omega$  and  $Q$  are determined from the phase-matching conditions, namely,  $Q = k_2 - k_1$ , and  $\Omega = \omega_2 - \omega_1$ , so that magnon mode transitions are permitted only for propagation in the forward (+x) direction. For the forward propagation, due to a mode transition, the dynamic magnetization in the perturbation magnetic field region can be expressed as a linear combination of the two coupled modes, i.e.

$$\mathbf{m}(x, y, t) = C_1 \mathbf{m}_1(x, y, t) + C_2 \mathbf{m}_2(x, y, t), \quad (2)$$

where  $\mathbf{m}_1$  and  $\mathbf{m}_2$  are the magnetization profiles of the eigenmodes in the absence of the perturbation field, and  $C_1$  and  $C_2$  the corresponding spin-wave amplitudes characterizing the mode transition.

Substituting Eq. (2) into the linearized Landau-Lifshitz-Gilbert equation, and based on the orthogonality of the eigenmodes, and the assumption of a slowly varying amplitude approximation, we obtain the following coupled-mode equations

$$\frac{d}{dx} \begin{pmatrix} C_1(x) \\ C_2(x) \end{pmatrix} = \begin{pmatrix} 0 & -iK/J_1 \\ -iK/J_2 & 0 \end{pmatrix} \begin{pmatrix} C_1(x) \\ C_2(x) \end{pmatrix}, \quad (3)$$

where the overlap integral  $K$  characterizes the coupling strength, and  $J_n \propto k_n$ . Given the initial conditions  $C_1(0) = 1$  and  $C_2(0) = 0$ , the solutions to Eq. (3) are

$$\begin{aligned} C_1(x) &= \cos(x\sqrt{a}) \\ C_2(x) &= -i\sqrt{J_1/J_2} \sin(x\sqrt{a}), \end{aligned} \quad (4)$$

where  $a = K^2/(J_1J_2)$ . For convenience, we introduce the coupling length  $l_c = \pi/(2\sqrt{a})$  which is defined to be the propagation distance over which one mode undergoes a complete transition to the other. The mode intensities calculated from Eq. (4) are shown in Figure 2a. Due to Gilbert damping, the intensities of modes along the  $x$ -direction of Figure 2a are modified by a factor  $e^{-x/\lambda}$ , where the spin-wave decay length[23]  $\lambda = v_g/[2\alpha\omega]$ ,  $v_g$  being the spin-wave group velocity and  $\alpha$  the Gilbert damping coefficient. The corresponding instantaneous profile of the  $z$ -component  $m_z$  of the dynamic magnetization is presented in the top panel of Figure 2b.

**Numerical simulations.** Micromagnetic simulations were performed to investigate the dynamics of the predicted spin-wave nonreciprocity by solving the Landau-Lifshitz-Gilbert equation. To determine the coupling length  $l_c$  (along the  $x$ -axis), the magnetic-field perturbation region was first chosen to be sufficiently long along the  $x$ -direction, i.e., for the occurrence of two complete mode transitions.

A continuous spin wave of mode  $[\omega_1, k_1]$  was excited at the left end of the waveguide as the initial wave. The simulated intensities  $|C_1|^2$  and  $|C_2|^2$  of the respective modes  $[\omega_1, k_1]$  and  $[\omega_2, k_2]$  as a function of interaction distance within the perturbation region, obtained by performing a fast Fourier transform of the out-of-plane component  $m_z$  of the dynamic magnetization in time, are displayed in Figure 2a. The simulated data accord well with the coupled-mode theory in terms of both the relative mode intensities and the coupling length. Both methods indicate that the energy is transferred back and forth between the coupled modes, with complete transfers occurring at integral multiples of the coupling length. The simulated instantaneous dynamic magnetization, presented in the bottom panel of Figure 2b, well reproduces the prediction of the coupled-mode model (top panel of Fig. 2b). It can be seen from Figure 2b that the forward-propagating mode undergoes a transition, with the symmetry of its  $m_z$  profile progressively evolving from even to odd and finally reverting to even.

To demonstrate the concept of nonreciprocal mode transitions, in the following simulations, the length of the perturbation region along the  $x$ -axis was set to the simulated coupling length  $l_c$ . Frequencies and propagation directions of the initial wave were varied by changing the frequency and location (left or right end of the waveguide) of the excitation

field. The snapshot of  $m_z$ , presented in Figure 3a, reveals that the symmetry of the mode profile of the right-propagating spin wave is completely converted from even to odd. The right panel of Figure 3a shows that the corresponding frequency spectrum changes from  $\omega_1$  to  $\omega_2$  after passing through the perturbation region. In contrast, on reversal of the propagation direction, i.e., when spin waves of mode  $[\omega_1, -k_1]$  were considered, no changes in their mode profiles or frequencies were found (Fig. 3b), indicating the occurrence of negligible mode transition. Thus, the waveguide exhibits time-reversal symmetry breaking, resulting in drastic contrasting effects for the two opposite propagation directions. Interestingly, the same nonreciprocal effects were also observed for the initial modes  $[\omega_2, k_2]$  and  $[\omega_2, -k_2]$  as illustrated in Figure 3c, d.

## Discussion

We have developed a coupled-mode model for exchange spin waves for analyzing spin-wave dynamics under a perturbation magnetic field. Employing this model, we demonstrated that application of the field can effect nonreciprocal spin-wave interband transitions arising from the simultaneous destruction of time-reversal and spatial-inversion symmetry. Micromagnetic simulations yielded results which accord well with those of the coupled-mode theory. The small discrepancy is partially ascribed to the neglect of dipolar interaction in the theory. Importantly, this spin-wave nonreciprocity could be exploited to design and fabricate unidirectional magnonic nanoscale devices, which are building blocks of integrated magnonic and spintronics circuits. For instance, when used in conjunction with spin-wave filters[29] to filter out the higher modes at  $\omega_2$ , the nonreciprocal waveguide will function as an isolator for spin waves of frequency  $\omega_1$ .

The nonreciprocity presented here has the following merits. First, it is based on nonreciprocal mode transitions due to a perturbation magnetic field, which differs from the previously reported magnonic nonreciprocity due to dipole-dipole interactions. As the phenomenon is valid for exchange-dominated spin waves, it could in principle permit the realization of nanoscale integrated magnonic circuits. Second, the linearity of the phenomenon makes its realization more straight-forward and energy-efficient than that involving nonlinear effects. Recently, it was reported that ultrafast dynamic control of photonic[30, 31] and magnonic structures[15, 17] offers linear approaches for realizing novel functionalities, such as frequency shift of waves, which usually involve the nonlinear effects

in static artificial materials, i.e. those with time-invariant structural arrangements. We have shown, from another perspective, that the dynamic modulation of a magnonic waveguide can realize hitherto unreported nonreciprocal propagation of spin waves. Third, in principle, the nonreciprocity is applicable to other isotropic ferromagnetic materials besides the material Permalloy used.

Dynamic control of photonic structures relies on ultrafast variation in the refractive index of materials[31], which is still a challenge and is often realized by utilizing nonlinear optical effects. In contrast, achieving dynamic control is much simpler and more straightforward in magnonics[17]. Because the effective field in the Landau-Lifshitz-Gilbert equation plays a similar role to the refractive index in Maxwell's equations, dynamic control of the effective field in magnonic structures is achievable simply through the application of an external magnetic field without involving nonlinear effects, as was done in this study. Analogous to the dynamic control in photonics, the topic of dynamic control of magnonic systems is of scientific interest and has enormous applications potential.

## References

- [1] K. Gallo *et al.*, Applied Physics Letters **79**, 314 (2001).
- [2] S. Manipatruni, J. T. Robinson, and M. Lipson, Physical Review Letters **102**, 213903 (2009).
- [3] Z. Yu, and S. Fan, Nat Photon **3**, 91 (2009).
- [4] S. J. B. Yoo, Nat Photon **3**, 77 (2009).
- [5] V. Grigoriev, and F. Biancalana, New Journal of Physics **12**, 053041 (2010).
- [6] C. R. Doerr, N. Dupuis, and L. Zhang, Opt. Lett. **36**, 4293 (2011).
- [7] M. S. Kang, ButschA, and P. S. J. Russell, Nat Photon **5**, 549 (2011).
- [8] M. Hafezi, and P. Rabl, Opt. Express **20**, 7672 (2012).
- [9] H. Lira *et al.*, Physical Review Letters **109**, 033901 (2012).
- [10] J. Y. Chin *et al.*, Nat Commun **4**, 1599 (2013).
- [11] P. K. Amiri *et al.*, Applied Physics Letters **91**, 062502 (2007).
- [12] K. Sekiguchi *et al.*, Applied Physics Letters **97**, 022508 (2010).
- [13] B. Li, L. Wang, and G. Casati, Physical Review Letters **93**, 184301 (2004).
- [14] X.-F. Li *et al.*, Physical Review Letters **106**, 084301 (2011).
- [15] A. D. Karenowska *et al.*, Physical Review Letters **108**, 015505 (2012).
- [16] H. Kurebayashi *et al.*, Nat Mater **10**, 660 (2011).
- [17] A. V. Chumak *et al.*, Nat Commun **1**, 141 (2010).
- [18] B. Lenk *et al.*, Physics Reports **507**, 107 (2011).
- [19] Z. K. Wang *et al.*, Physical Review Letters **94**, 137208 (2005).
- [20] Y. Kajiwara *et al.*, Nature **464**, 262 (2010).
- [21] T. Liu, and G. Vignale, Physical Review Letters **106**, 247203 (2011).
- [22] Z. Wang *et al.*, Physical Review Letters **107**, 146602 (2011).
- [23] MadamiM *et al.*, Nat Nano **advance online publication** (2011).
- [24] S. O. Demokritov *et al.*, Nature **443**, 430 (2006).
- [25] T. An *et al.*, Nat Mater **advance online publication** (2013).
- [26] R. E. Camley, Surface Science Reports **7**, 103 (1987).
- [27] C. Mathieu *et al.*, Physical Review Letters **81**, 3968 (1998).
- [28] J. N. Winn *et al.*, Physical Review B **59**, 1551 (1999).
- [29] F. Ciubotaru *et al.*, Journal of Physics D: Applied Physics **45**, 255002 (2012).
- [30] Y. Tanaka *et al.*, Nat Mater **6**, 862 (2007).
- [31] J. Bravo-Abad, and M. Soljacic, Nat Mater **6**, 799 (2007).

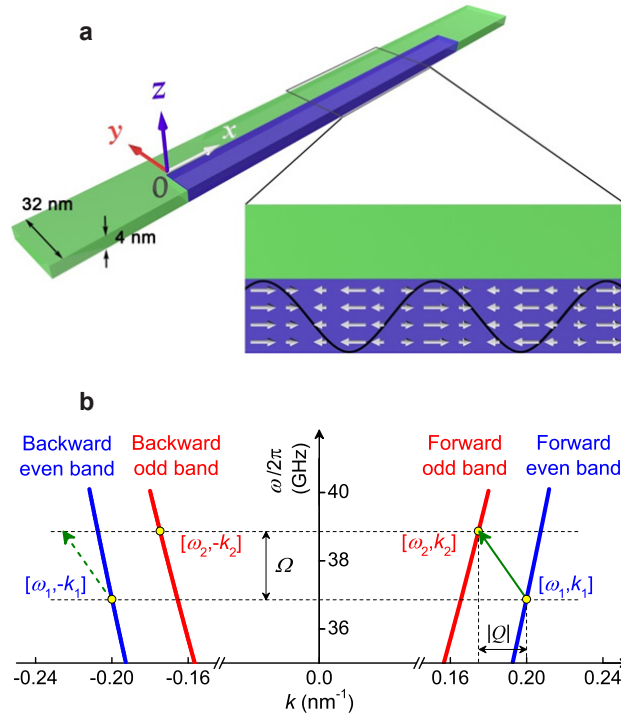


**Figure 1 | Principles of nonreciprocal spin-wave mode transitions in the Permalloy nanostripe waveguide.** (a) Schematics of the Permalloy nanostripe waveguide. The perturbation magnetic field  $h'(x, y, t) = h_0(y) \cos(Qx - \Omega t)$  is applied in the  $x$ -direction within the blue region. The enlarged view shows the instantaneous profile of the magnetic perturbation field vectors represented by arrows. The wave profile of the perturbation field is traveling in the  $-x$  direction; (b) Dispersion relations of spin waves for the range considered with blue and red lines representing the even and odd symmetry bands, respectively. The solid (dashed) green arrow indicates shifts of frequency and wavevector in the forward (backward) propagation direction due to the perturbation magnetic field. Resonant coupling exists between modes  $[\omega_1, k_1]$  and  $[\omega_2, k_2]$  in the forward ( $+x$ ) direction, while coupling between modes  $[\omega_1, -k_1]$  and  $[\omega_2, -k_2]$  in the backward ( $-x$ ) direction is insignificant.

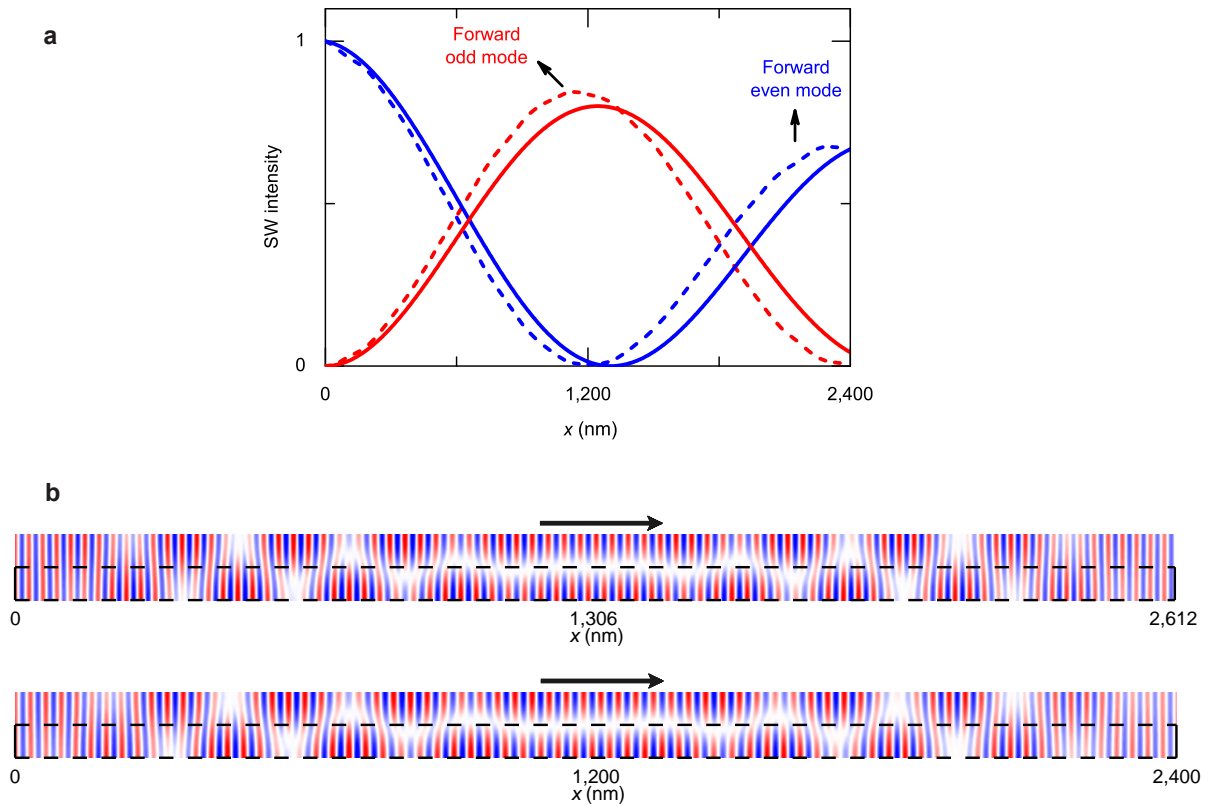


**Figure 2 | Forward spin-wave mode transitions in the waveguide.** (a) Intensities of two coupled magnon modes  $[\omega_1, k_1]$  (red curves) and  $[\omega_2, k_2]$  (blue curves) obtained from the coupled-mode model (solid curves) and micromagnetic simulations (dashed curves), respectively; (b)  $x$ - $y$  view of instantaneous dynamic magnetization  $m_z$  based on the coupled-mode theory (top panel) and micromagnetic simulations (bottom panel). Dashed boxes denote the regions where the perturbation field is applied. Transitions between the two modes result in the mode profiles (across the waveguide width) to gradually evolve, with increasing  $x$ , from being even to odd and back to even symmetry. The coupling length is determined to be 1306 and 1200 nm based on the coupled-mode theory and the micromagnetic simulations, respectively. The magnitudes of  $m_z$  are color-coded, with red, white and blue representing positive maximum, zero and negative maximum, respectively. The arrows indicate the propagation of the two modes in the forward ( $+x$ ) direction.

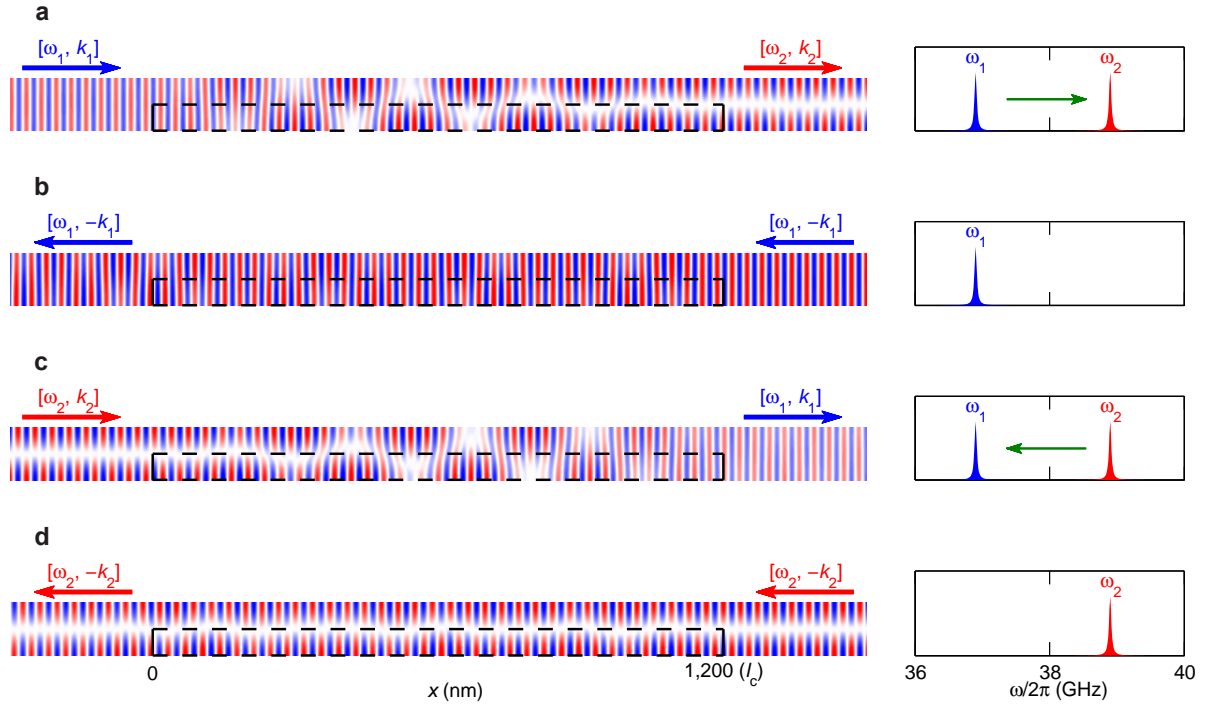


**Figure 3 | Snapshots of the out-of-plane components  $m_z$  of spin waves with different initial mode profiles and propagation directions in the waveguide. (a)** Spin-wave mode  $[\omega_1, k_1]$  propagating from left to right undergoing a complete transition to mode  $[\omega_2, k_2]$ ; **(b)** Spin-wave  $[\omega_1, -k_1]$  propagating from right to left remaining unaltered; **(c)** Spin-wave  $[\omega_2, k_2]$  propagating from left to right undergoing a complete transition to mode  $[\omega_1, k_1]$ ; **(d)** Spin-wave  $[\omega_2, -k_2]$  propagating from right to left remaining unaltered. The corresponding mode frequency changes for the four cases are indicated by panels on the right. Dashed boxes denote regions where the perturbation field is applied.